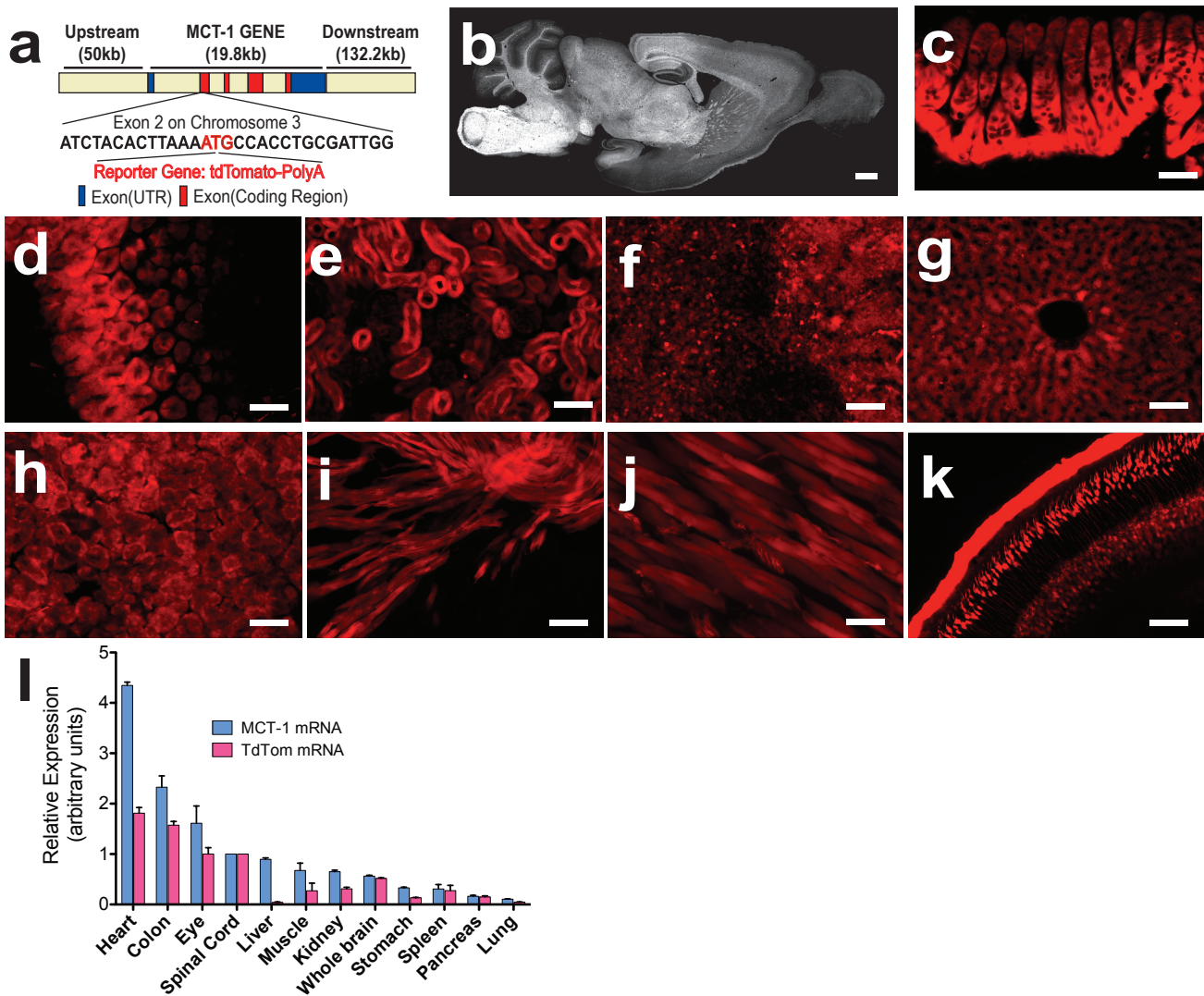


Supplementary Figure 1: Schematic of lactate supply to axons.

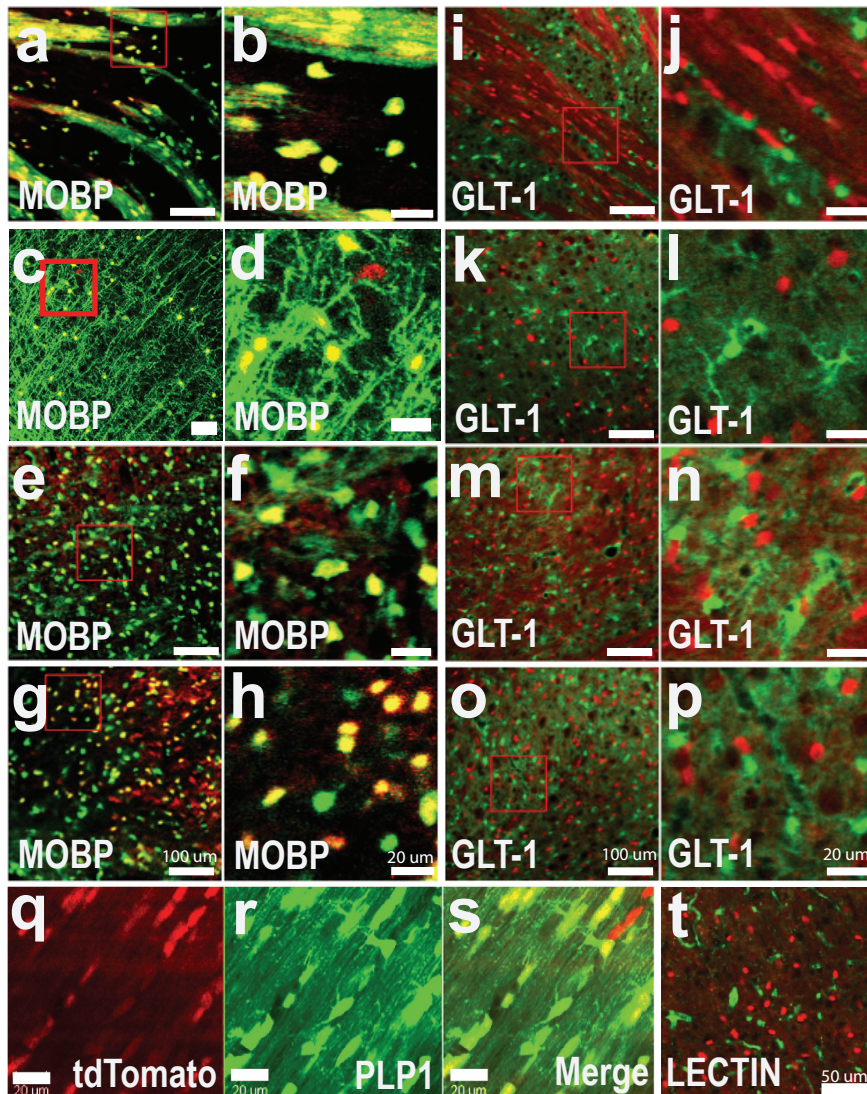
Oligodendroglia support axons and neurons by delivering lactate via MCT1 directly to axons, initial axon segments and possibly somas in gray matter. The metabolic supply of oligodendroglial lactate may come from gap junction-coupling between oligodendroglia and astroglia, which produce metabolic precursors from glycogen and their contacts with the vasculature.

Modified from Fünfschilling et. al, Nature 485, 517–521 (24 May 2012).



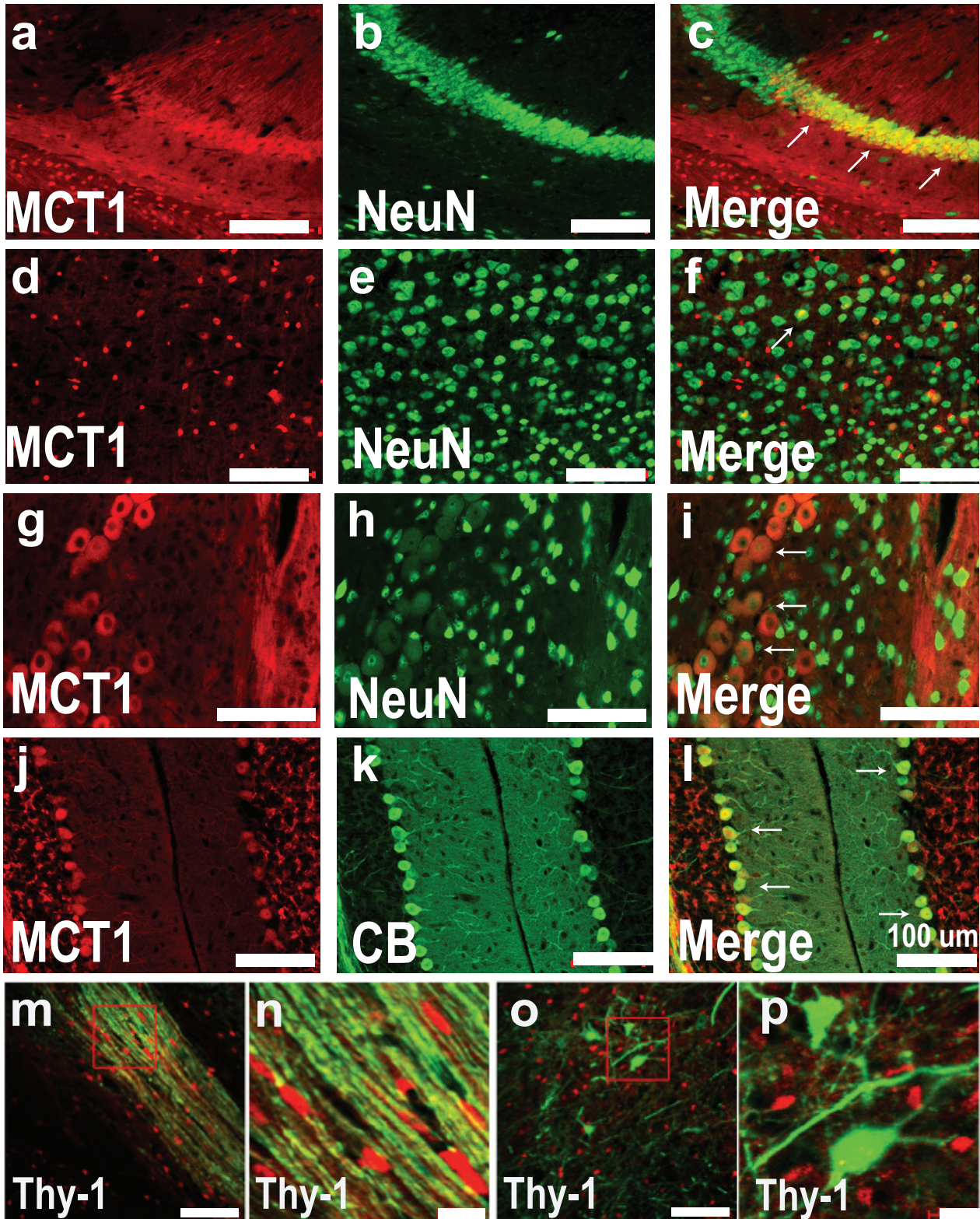
Supplementary Figure 2: Low power brain and non-CNS localization of MCT1 in reporter mice.

(a) MCT1 td-Tomato reporter construct used for producing BAC transgenic mice. (b) MCT1 tdTomato fluorescence in a sagittal section of the brain from a MCT1 BAC reporter mouse (scale bar = 0.7 mm). (c-k) Photomicrographs of colon (c), stomach (d), kidney (e), spleen (f), liver (g), pancreas (h), heart (i), skeletal muscle (j), and retina (k) from tdTomato MCT1 reporter mice (scale bars = 50 μ m). (l) Real-time RT PCR quantification of MCT1 (blue) and tdTomato (pink) mRNA from various organs ($n=4$, error bars \pm S.E.M.).



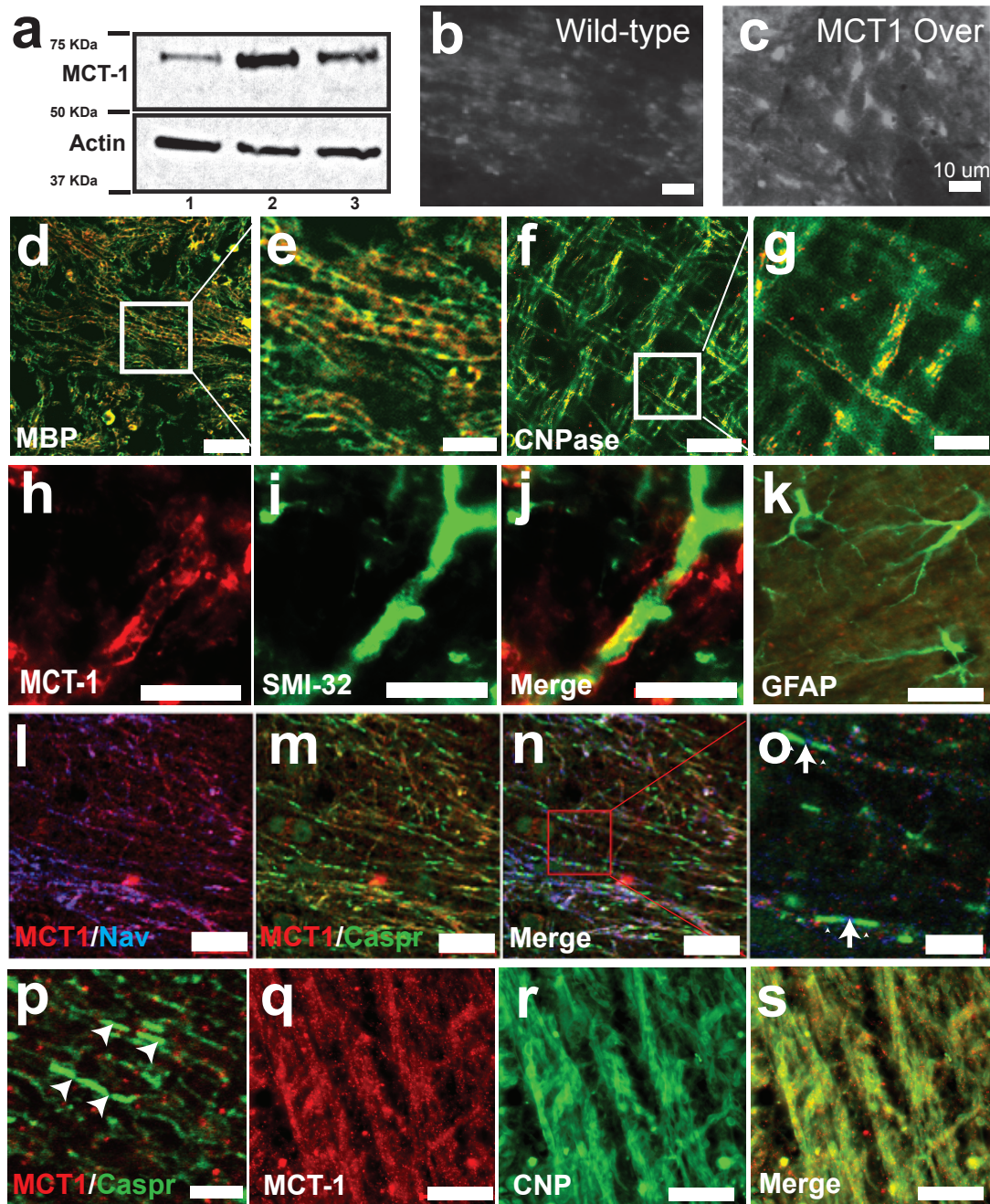
Supplementary Figure 3: MCT1 expression within oligodendrocytes, not astrocytes, in other brain regions.

(a-h) MCT1 reporter (red) co-localized with myelin-associated oligodendrocyte protein (MOBP) reporter (green) in striatum (a,b), cortex (c,d), brainstem (e, f), and cerebellar white matter (g, h). (i-p) MCT1 reporter NOT co-localized with GLT-1 in striatum (i, j), cortex (k, l), brainstem (m, n), and cerebellar white matter (o,p). (q-s) Optic nerves from MCT1 reporter mice crossed with eGFP proteolipid protein (PLP1) reporter mice. (t) Lectin-stained endothelial cells in the cortex of MCT1 reporter mice. Scale bars, 100 μm (a, c, e, g, i, k, m, o), 20 μm (b, d, f, h, j, l, n, p, q-s), 50 μm (t).



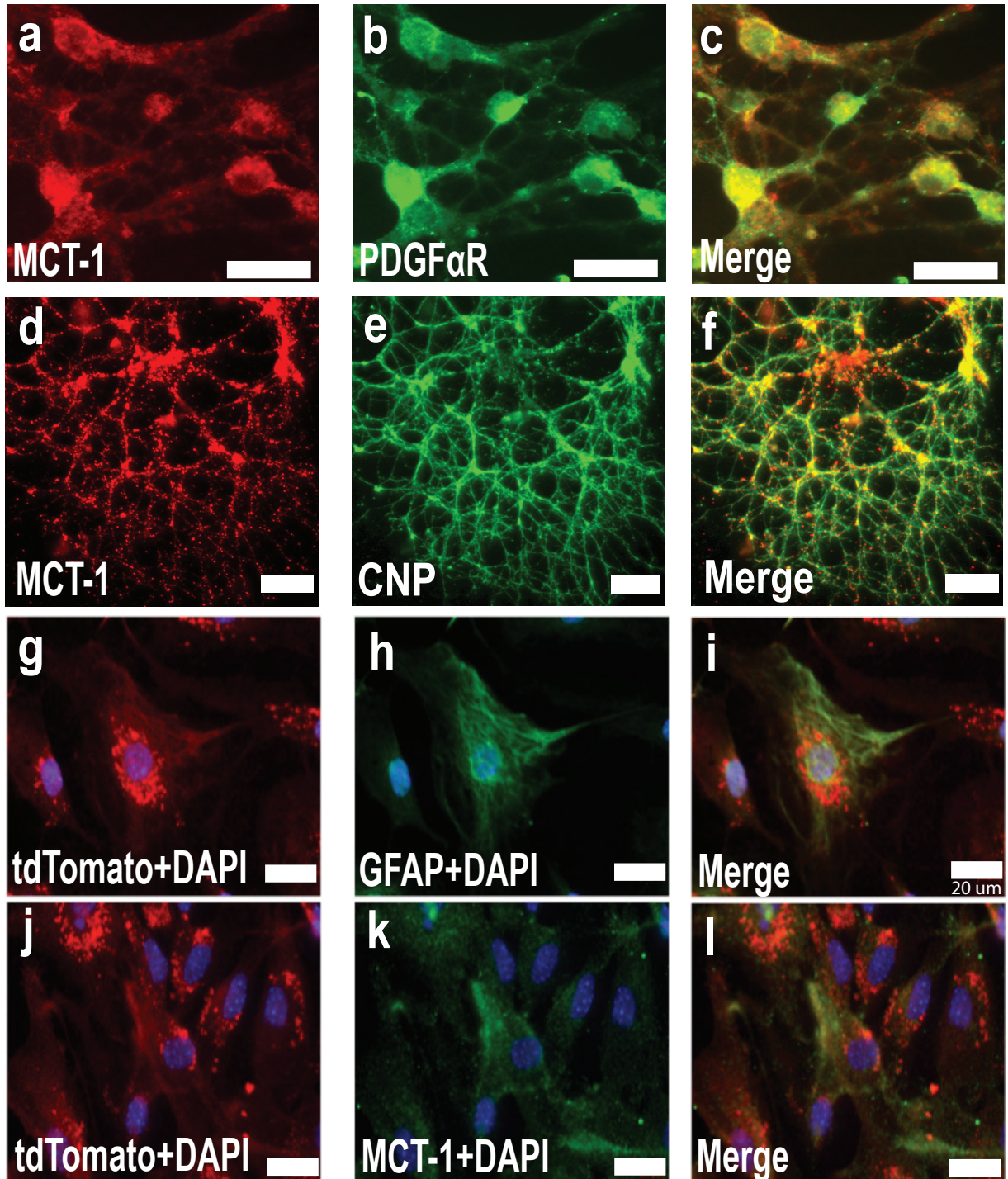
Supplementary Figure 4: MCT1 reporter expression in small subset of neurons.

(a-l) MCT1 reporter co-localized with NeuN in CA1 region of hippocampus (a-c; CA1 indicated by arrows), cortex (d-f; co-localized neuron indicated by arrow), brainstem trigeminal ganglion neurons (g-i; indicated by arrows), and cerebellar Purkinje neurons (j-l; indicated by arrows). (m-p) MCT1 reporter (red) was not colocalized with thy-1 (green) in the striatum (m,n) or the spinal cord (o, p). Scale bars, 100 μm (a-m, o), 20 μm (n, p).



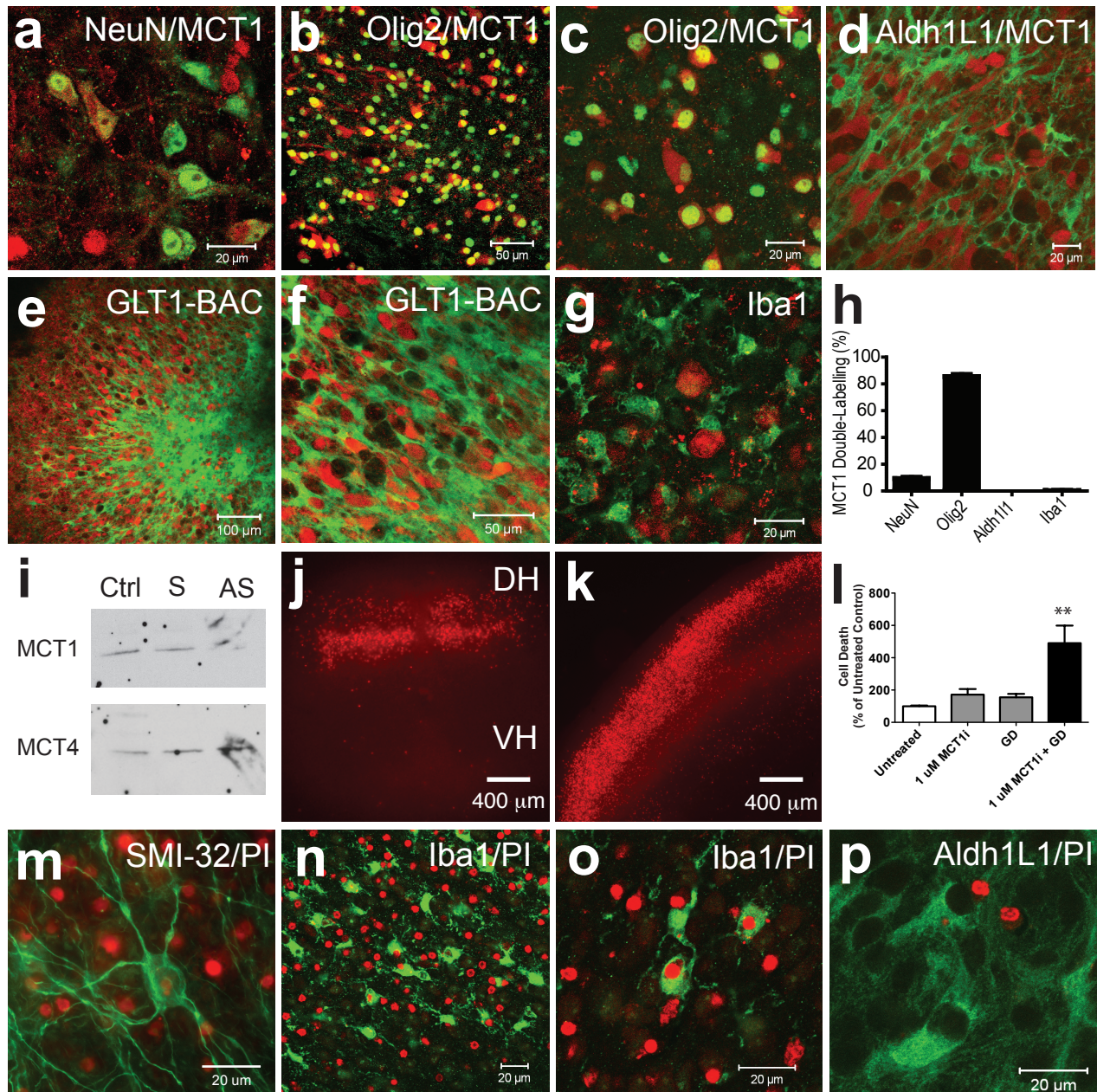
Supplementary Figure 5: Antibody localizes MCT1 to white matter and myelin surrounding axons.

(a) Western blot from wild-type (1) and 2 lines of MCT1 overexpressor mice (2,3). (b, c) MCT1 immunofluorescence in cortex from wild-type (b) and MCT1 over-expressor (c) mice. (d-g) Low (d,f) and high (e, g) magnification of MCT1 immunoreactivity co-localized with myelin and oligodendrocyte markers, MBP (d, e) and CNP (f, g). (h-j) MCT1 immunoreactivity (red) localized around, but not within, axons labelled by neurofilaments (green; SMI-32). (k) MCT1 immunoreactivity not co-localized with GFAP in the hippocampus. (l-o) Triple-labelled immunofluorescence for MCT1 (red), voltage-gated sodium channels (Nav; blue), and contactin-associated protein (Caspr; green) at low (l-n) and high (o) magnification. (p, q) Caspr (green)- and MCT1 (red)-immunoreactivity in the optic nerve. (r, s) Human cortical white matter immunostained for MCT1 and CNPase. Scale bars, 10 μ m (d, f, h-j), 5.6 μ m (e, g, o-q), 20 μ m (k, l-n, r, s).



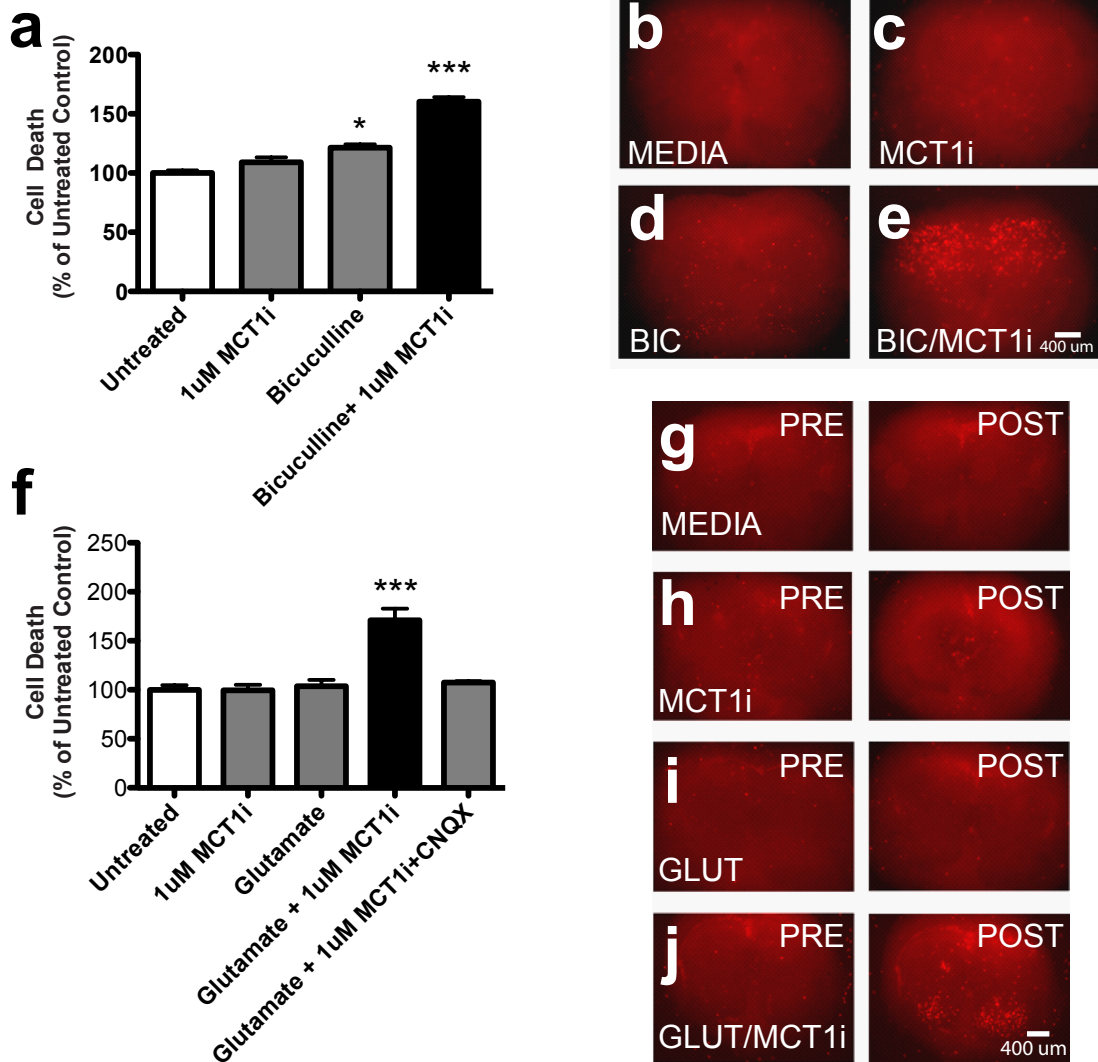
Supplementary Figure 6: Primary oligodendrocyte precursor, oligodendrocyte, and astrocyte cultures express MCT1.

(a-c) Primary oligodendrocyte precursor cultures from wild-type mice immunostained for MCT1 and PDGF α receptors. (d-f) MCT1 immunoreactivity within cultured oligodendrocyte. (g-l) Primary astrocyte cultures obtained from tdTomato MCT1 reporter mouse embryos immunostained for glial fibrillary acidic protein (GFAP; g-i) or MCT-1 (j-l). Scale bars, 20 μ m (a-c, g-l), 10 μ m (d-f).



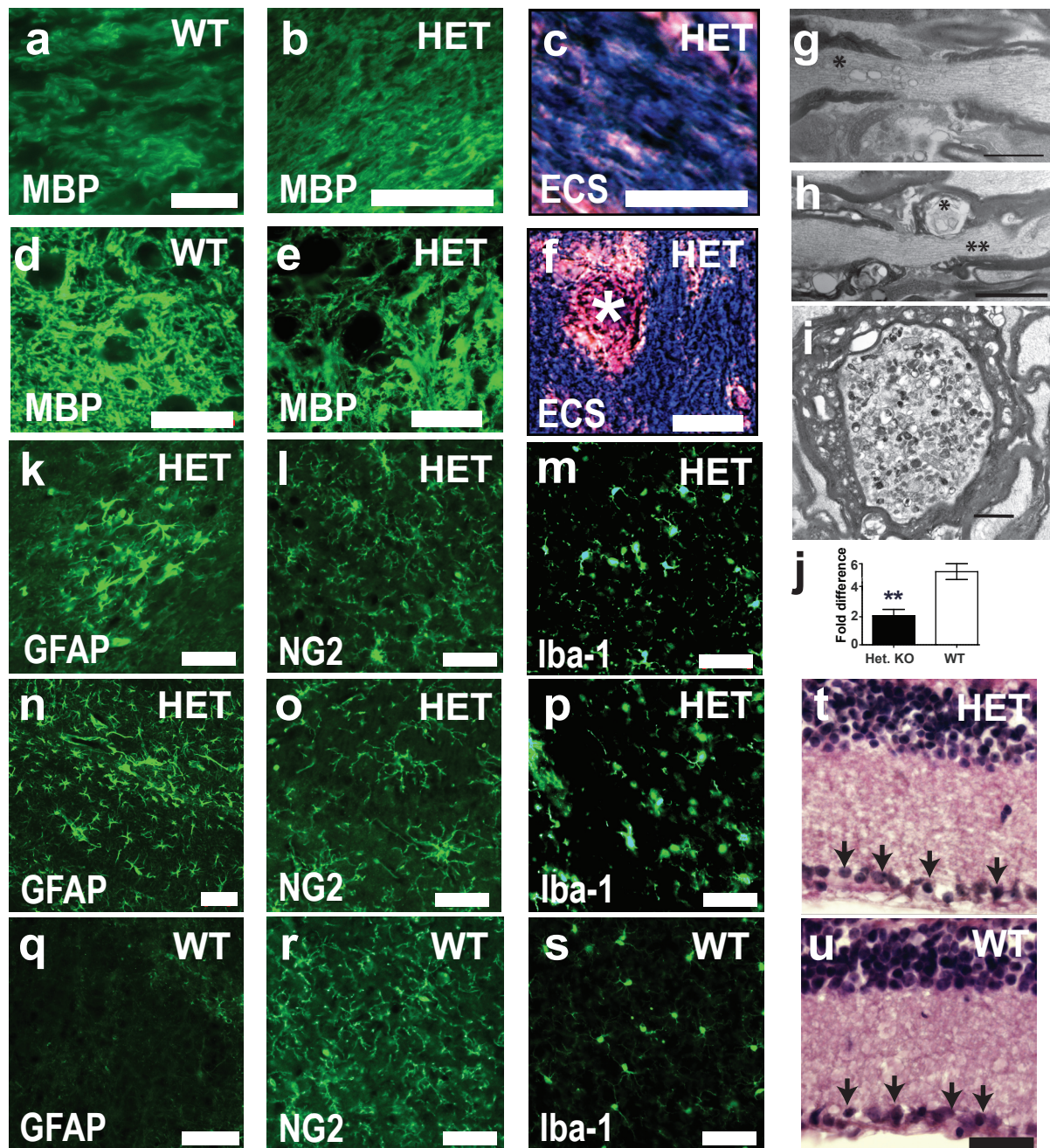
Supplementary Figure 7: Organotypic spinal cord cultures.

(a-g) Spinal cord organotypic cultures from MCT1 reporter (red) mice immunostained for NeuN (a; green), Olig2 (low power, b; high power, c), Aldh1L1 (d), or Iba1 (g). (e-f) Low (e) and high (f) power magnification of organotypic cultures produced from MCT1 (red) and GLT1 (green) double BAC reporter mice. (h) Percentage of MCT1 reporter positive cells immunoreactive for cell-specific markers ($n=5$ sections per group). (i) MCT1 and MCT4 Western blots of organotypic cultures treated with media (Ctrl), MCT1 sense oligonucleotides (Sense), and MCT1 anti-sense oligonucleotides (ASO). (j,k) Propidium iodide (PI) uptake in organotypic spinal cord (j) and cortical (k) cultures treated with MCT1i and glucose deprivation. (l) Graph of cell death, measured by PI uptake, in cortical organotypic cultures after treatment with buffer ($n=6$), MCT1i ($n=5$), glucose deprivation ($n=4$) or MCT1i plus glucose deprivation ($n=7$), normalized to untreated group. Double-labelling of PI in post-treatment organotypic spinal cord cultures with motoneuron (m), microglial (n, o), and astrocyte (p) markers. Scale bars, 20 μ m (a, c, d, g, m-p), 50 μ m (b, f), 400 μ m (j, k).



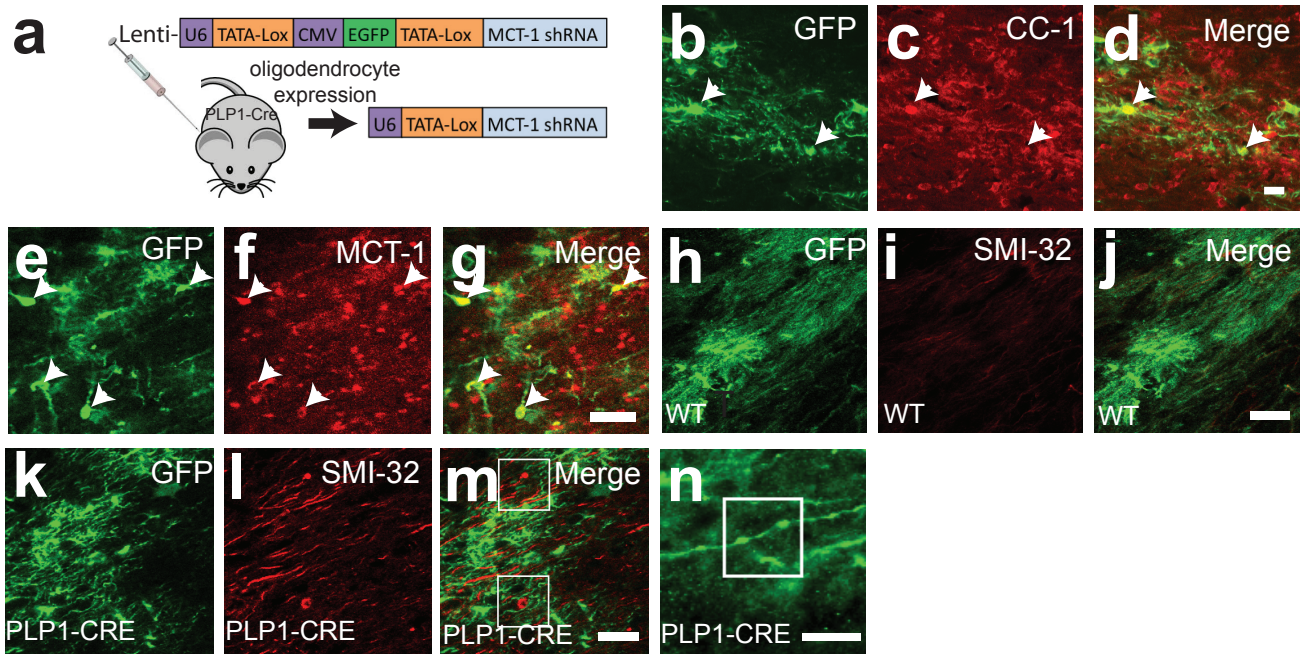
Supplementary Figure 8: Depolarization increases vulnerability to MCT1i.

(a) Propidium iodide (PI) quantification of cell loss in organotypic spinal cord cultures \pm bicuculline (100 μ M) for 3 days, \pm MCT1i ($n=28, 14, 23, 28$ for columns 1-4 respectively). (b-e) PI fluorescence in organotypic spinal cord cultures treated with media (b), MCT1i (c), bicuculline (d), or bicuculline plus MCT1i (e). (f) PI quantification of cell loss in organotypic spinal cord cultures \pm glutamate (250 μ M) for 1 hour, \pm MCT1i, or \pm glutamate antagonist, CNQX ($n=19, 13, 25, 33, 19$ for columns 1-5 respectively). (g-j) PI fluorescence in spinal cord cultures before (PRE) and after (POST) treatment with media (g), MCT1i (h), glutamate (i), or glutamate plus MCT1i (j). Error bars \pm S.E.M. * $p < 0.05$, *** $p < 0.001$



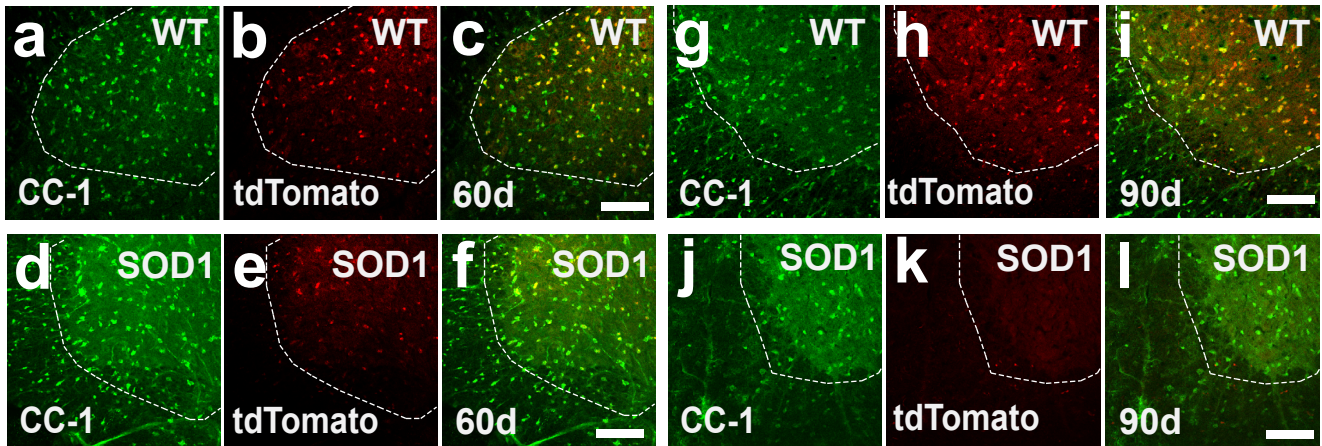
Supplementary Figure 9: Other pathology in MCT1 heterozygote null mice.

(a-f) Myelin basic protein (MBP) immunoreactivity (a-b, d-e) and eriochrome staining (c, f; ECS) unchanged in the optic nerve (a-c) and spinal cord (d-f, motoneuron indicated by asterisk) from MCT1 heterozygote null (HET) compared to wild-type (WT) mice. (g) In longitudinal electron microscopic (EM) sections of optic nerve, most paranodes have normal morphology (g, h), even around early degenerating axons (asterisk); however, a few paranodes in degenerating axons (h; double asterisk) show features of degeneration themselves (asterisk). (i) Multi-vesicular body in the spinal cord of HET mice. (j) Real-time RT PCR of MCT1 mRNA expression in 1 year old spinal cords from HET mice and littermate WT mice ($n=4$). (k-s) Glial fibrillary acidic protein (GFAP), NG2, and Iba-1 immunoreactivity in the cortex (k-m) and hippocampus (n-p) of HET or cortex of WT (q-s) mice. (t, u) No loss of retinal ganglion cells (arrows) in MCT1 heterozygote null mice (t), compared to wild-type mice (u). Scale bars, 20 μm (a-c), 50 μm (d-f, k-s, t, u), 1 μm (g, h), 2 μm (i).



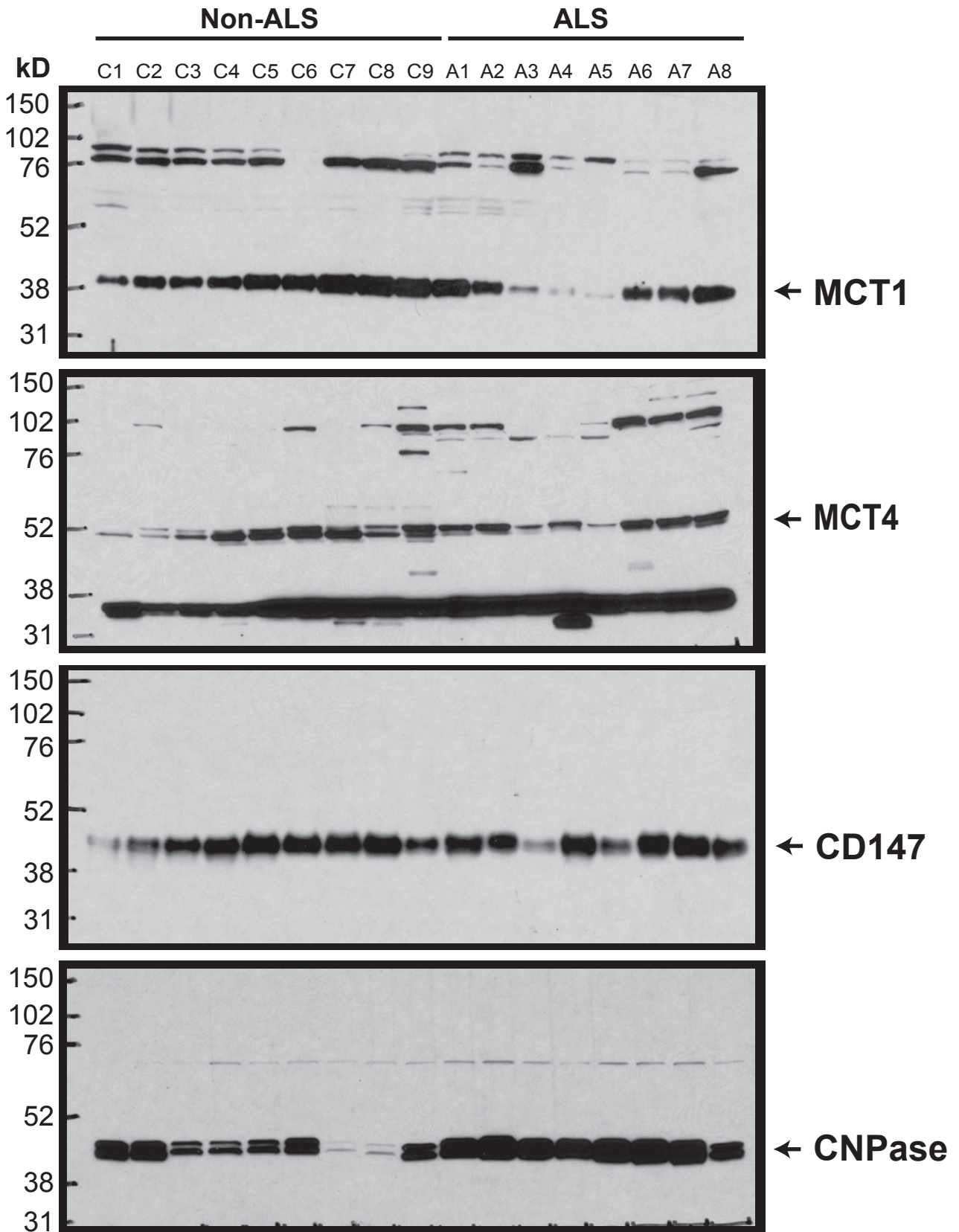
Supplementary Figure 10 : Selective downregulation of MCT1 in oligodendrocytes within the corpus callosum produces axon degeneration.

(a) Cre recombinase-dependent lentivirus, which transcribes shRNA in Cre expressing cells, was injected into the corpus callosum of PLP1-Cre mice that express Cre only within oligodendrocytes in the brain. (b-g) Lentivirus injected into MCT1 reporter mice demonstrates capacity to transfect CC-1 positive (b-d) or MCT1 positive (e-g) oligodendrocytes (Arrowheads). (h-j) Normal low level immunoreactivity to non-phosphorylated neurofilaments (SMI-32) following virus injection into corpus callosum of wild-type mice. (k-m) Increased expression of SMI-32 and development of axonal swellings (boxed areas in m) in corpus callosum following injection of virus into PLP1-Cre mice. (n) GFP infrequently labels axons in the corpus callosum in PLP1-Cre mice and occasional axon swellings can be seen following treatment with lentivirus that downregulates MCT1 within oligodendrocytes. (Note: when injected into PLP1-Cre mice treated with tamoxifen, the lentivirus GFP is excised in oligo-dendrocytes, so specific cellular localization is uncommonly seen). Scale bars, 10 μ m (b-g, n), 20 μ m (h-m).

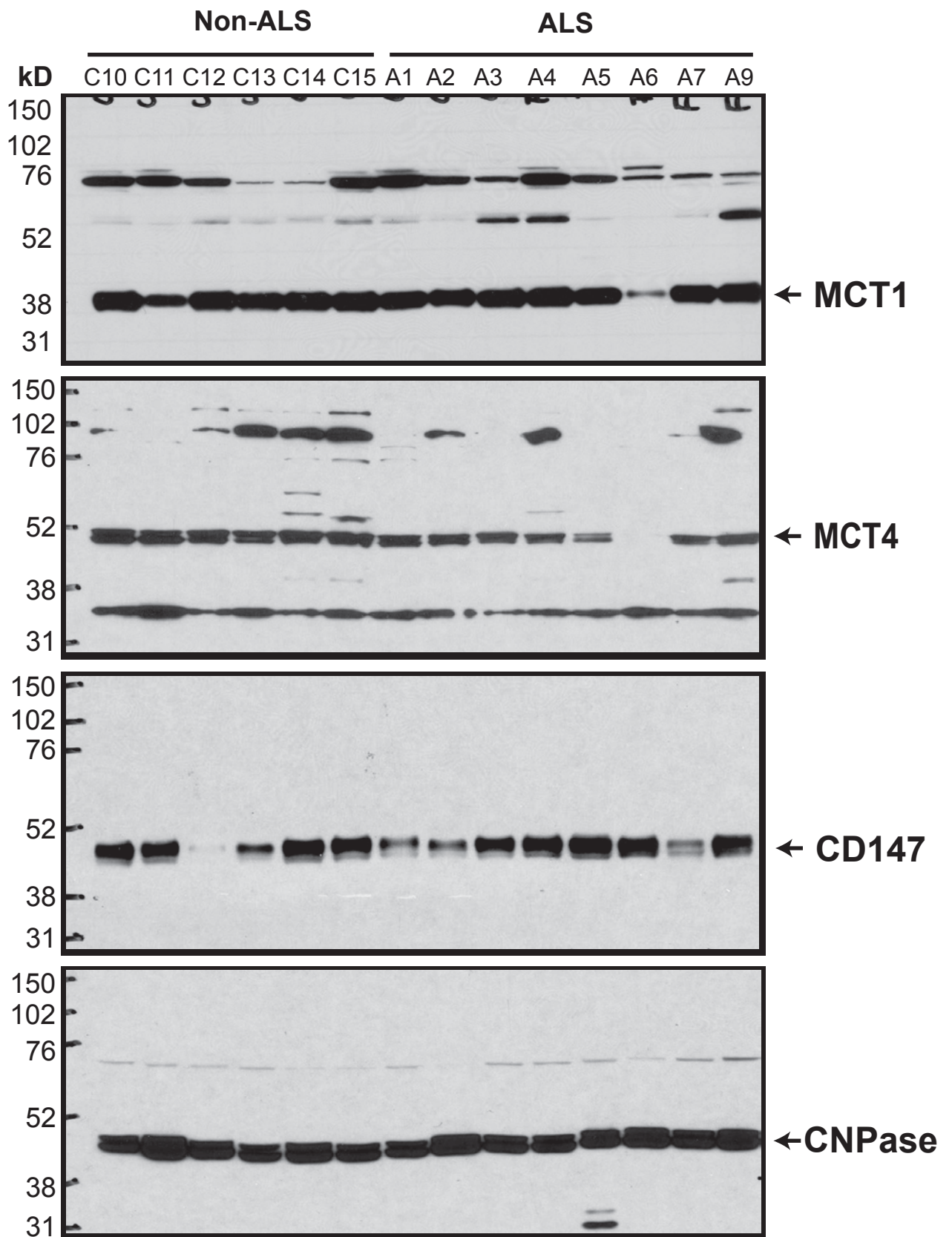


Supplementary Figure 11: MCT1 Reporter activity in the spinal cord from early and presymptomatic G93A SOD1 transgenic mice.

Ventral horn of the spinal cord from 60 (a-f) and 90 (g-l) day old SOD1 transgenic mice (d-f; j-l) and littermate controls (a-c; g-i) immunostained with the oligodendrocyte marker CC-1. Boundaries of ventral horn grey matter marked by dashed line (scale bars = 100 μ m).



Supplementary Figure 12: Full Western blots of human motor cortex from ALS and non-ALS patients. Labels correspond to patient characteristics in Table 1.



Supplementary Figure 13: Full Western blots of human frontal cortex from ALS and non-ALS patients. Labels correspond to patient characteristics in Table 1.

Supplementary Table 1. Patient demographics for autopsy samples used in Western blots

Patients with Amyotrophic Lateral Sclerosis

Patient ID	Age of Death	Gender	Race	Site of Onset	Duration	Motor Cortex	Frontal Cortex
A1	64	Male	Caucasian	UE	1 year	XX	XX
A2	68	Female	Caucasian	UE	5 years	XX	XX
A3	61	Female	Caucasian	LE	4 years	XX	XX
A4	65	Male	Caucasian	LE	3 years	XX	XX
A5	45	Female	Caucasian	LE	3 years	XX	XX
A6	49	Male	Caucasian	UE	4 years	XX	XX
A7	72	Female	Caucasian	Bulbar	2 years	XX	XX
A8	47	Male	Caucasian	LE	3 years	XX	
A9	69	Male	Caucasian	Unknown	2 years		XX

Patients without Amyotrophic Lateral Sclerosis

Patient ID	Age of Death	Gender	Race	Motor Cortex	Frontal Cortex
C1	79	Female	Caucasian	XX	
C2	86	Female	Black	XX	
C3	62	Male	Caucasian	XX	
C4	45	Female	Caucasian	XX	
C5	59	Male	Caucasian	XX	
C6	66	Male	Caucasian	XX	
C7	59	Male	Caucasian	XX	
C8	70	Male	Caucasian	XX	
C9	79	Male	Caucasian	XX	
C10	59	Male	Caucasian		XX
C11	74	Male	Caucasian		XX
C12	91	Female	Caucasian		XX
C13	47	Male	Caucasian		XX
C14	48	Female	Black		XX
C15	79	Male	Caucasian		XX